Atmospheric Environment 60 (2012) 25–36

Contents lists available at SciVerse ScienceDirect

Atmospheric Environment

journal homepage: www.elsevier.com/locate/atmosenv

Impacts of land use changes and synoptic forcing on the seasonal climate over the Pearl River Delta of China

Camilla K.M. Cheng [a,*], Johnny C.L. Chan [a,b]

[a] School of Energy and Environment, City University of Hong Kong, Tat Chee Avenue, Kowloon, Hong Kong
[b] Guy Carpenter Asia-Pacific Climate Impact Centre, City University of Hong Kong, Hong Kong

HIGHLIGHTS

- ► Urban warming and modifications of surface variables are more pronounced in summer.
- ► Summer rainfall is enhanced but winter precipitation is reduced.
- ► The local forcing dominates over the large-scale forcing in summer but the reverse is true in winter.
- ► A strong synoptic flow can reduce the urbanization effects over an urban area.

ARTICLE INFO

Article history:
Received 18 January 2012
Received in revised form
13 May 2012
Accepted 4 June 2012

Keywords:
Urbanization
Seasonal climate
Urban rainfall

ABSTRACT

In this study, the impact of the rapid rate of urbanization over the Pearl River Delta (PRD) region of China since the 1980s on its seasonal climate is investigated using the Weather Research and Forecasting Model. Two land-cover data are employed to simulate the urbanization effects on the regional climate in both summer (June and August) and winter (December and February) for 26 years from 1984 to 2009. Spatial and temporal features of the urbanization effect on temperature and precipitation are found to be different between summer and winter. Urban warming and modifications of surface variables such as surface latent heat flux and 2-m relatively humidity are more pronounced in summer. Moreover, summer rainfall is enhanced but winter precipitation is reduced. The increase in summer rainfall is mainly contributed by the strong urban heat island effect, which enhances the convective circulation over the urban area. On the other hand, a reduction in winter precipitation is observed. The different behavior during winter time is due to drier northerly winds and increased atmospheric stability. Furthermore, the changes in winter precipitation are associated with the synoptic forcing such as El Niño – Southern Oscillation and monsoon, but no significant correlation can be found between changes in summer rainfall and the synoptic forcing. In other words, the local surface forcing (including radiative fluxes, heat, momentum and water transfer at the air–land interface) dominates over the synoptic forcing in summer but the reverse is true in winter. Under conditions of weak synoptic flow, local thermodynamic effects of urbanization dominates, setting up convergence zone over the urban area and leading to increased precipitation. However, during winter time, under the influence of strong northeasterly synoptic flow, dynamic effects of increased surface roughness urban areas dominate and lead to convergence upwind of the urban region.

1. Introduction

Urbanization is considered as one of the important change of land use in the 20th century. The urban growth in developing countries such as China was projected to be on an unprecedented scale in the next few decades (UNFPA, 2007). Therefore, problems associated with urbanization must be addressed. A growing number of research papers on urban climatology have been published in recent years. The objectives of these urban climate studies vary from investigating the underlying physics, chemistry and biology of the urban atmosphere; developing operational weather forecasting skills; and examining environmental sustainability and policy planning.

Although studies have mostly been directed at the anthropogenic influences of the atmospheric composition changes, modifications of land use have also been found to have significant impacts on the regional climate. Researchers found that changes in physical

* Corresponding author.
E-mail address: kamcheng5@student.cityu.edu.hk (C.K.M. Cheng).

1352-2310/$ – see front matter © 2012 Elsevier Ltd. All rights reserved.
http://dx.doi.org/10.1016/j.atmosenv.2012.06.019

properties of land surface alter the surface energy balance above the surface, hence inducing urban warming (Tayanç and Toros, 1997), storm and cloud enhancement (Niyogi et al., 2011; Shem and Shepherd, 2008; Inoue and Kimura, 2004) and rainfall anomalies (Kishtawal et al., 2009; Huff and Changnon, 1972; Kalnay and Cai, 2003) over urban areas.

The Pearl River Delta (PRD) region, a special economic zone located in southeastern China, has been one of the fastest developing regions in the world since the 1980s (Fig. 1). A considerable loss of cropland and expansion in urban or built-up land over the PRD region has been observed (Seto and Kaufmann, 2009). Due to this rapid urbanization in recent decades, PRD has been a region of great research interest to urban climatologists. Studies show that urbanization contributes to an increase in surface temperature due to land use changes (Zhang et al., 2005; Chen et al., 2010; Lam, 2006). A study of urban modification of the local circulation over PRD also found that the urban heat island effect (UHI) increased air temperature gradient between urban area and the nearby ocean causing an enhancement in the land–sea breeze circulation (Lo et al., 2007).

While urban warming is well-documented, the urbanization effect on regional rainfall still remains uncertain. By using satellite images and precipitation data from 16 meteorological stations in the PRD, a causal relationship was found between urban land use and reduced rainfall over the urban area in dry winter seasons, but not in summer (Kaufmann et al., 2007). In other words, urbanization effect on the rainfall over the PRD region appears to be seasonal. Moreover, as the rainfall over the PRD region is found to be sensitive to the monsoons and the El Niño-Southern Oscillation (ENSO, Zhou et al., 2010), the lack of clearly-observable urbanization impacts in this region may be due to the domination of the synoptic atmospheric factors over the effect of land surface changes. In addition, the underlying mechanisms of the observed variation still have not been revealed.

Because of these possibilities, it is hard to isolate the urbanization impacts on regional climate from statistical analyses of observed meteorological data. Sensitivity tests through numerical modeling are therefore useful in isolating the contribution of each forcing from urbanization, which is the approach adopted in this study. The objectives of the current study are therefore to quantify the urbanization impacts on the climate over the PRD and reveal the underlying mechanisms causing the regional climate changes using a numerical model. These results will help determine the urbanization impact on the climate for different seasons and the relative importance of the synoptic forcing compared with that due to urbanization over the PRD region.

2. Data, model and methodology

2.1. Weather Research and Forecasting (WRF) Model

The WRF model is a non-hydrostatic model with a mass-coordinate system (Skamarock et al., 2005). The National Centers for Environmental Prediction 2.5° latitude/longitude resolution global reanalysis data (NNR) are used for the atmospheric initial and lateral boundary conditions. In the current study, a single model domain is used instead of grid nesting approach to avoid distortion of information traveling through the boundaries of nested grids and spurious oscillations at grid interface that may cause unrealistic performance throughout the domain. Moreover, to balance between the computational time and capturing localized surface features, an optimal domain is selected, which consists of 80 × 80 grid points with 20 km horizontal grid spacing and 28 vertical sigma levels (Fig. 2). However, the limitation of the simulation would mostly be caused by the abrupt change from the driving data to the model input data that may not able to resolve the smaller-scale features forced by the surface boundary (Castro et al., 2005). The Kain–Fritsch cumulus

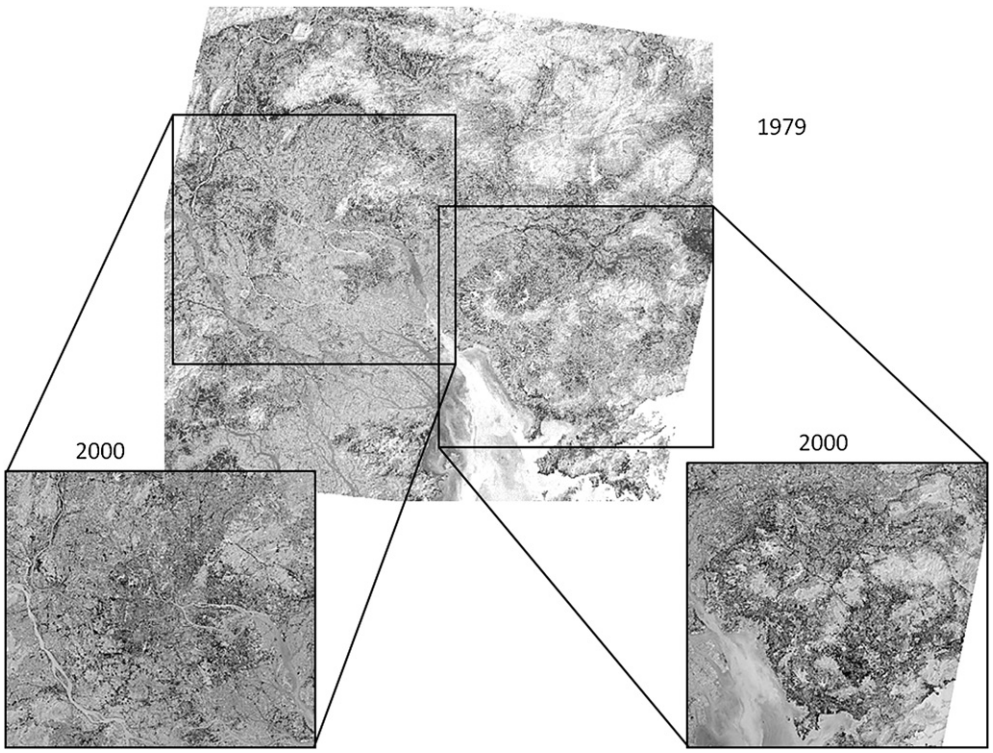

Fig. 1. Land use and land cover of PRD region in 1979 (large) and 2000 (small) observed by NASA's Landsat 3 (NASA, 1979) and Landsat 7 (NASA, 2000), respectively.

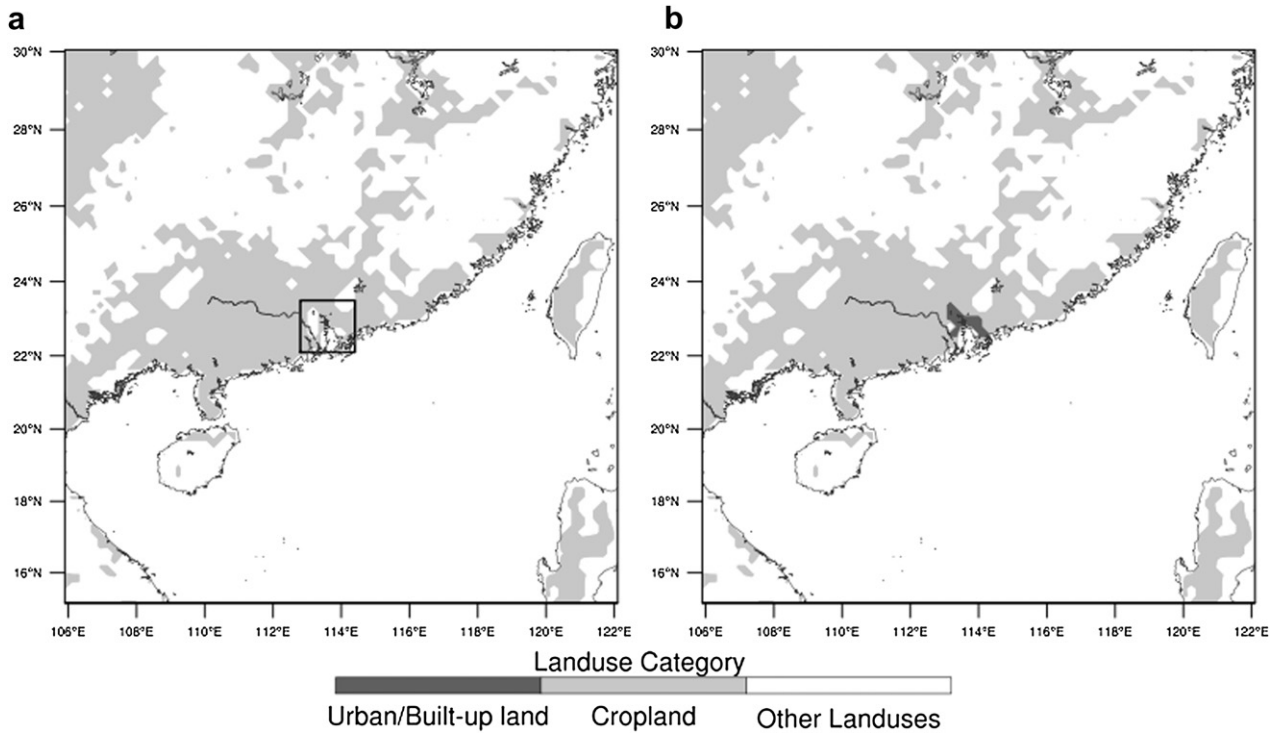

Fig. 2. a) The model domain for simulation with the box showing the location of PRD region. A total of 80 × 80 grid points with 20 km horizontal grid spacing. The land cover based on the USGS 24-category vegetation data in 1993. b) The land cover based on the HKPD land use data in 2003. The light gray color represents the irrigated cropland; dark gray color represents the urban or built-up areas and white color represents other types of land use.

parameterization scheme (Kain and Fritsch, 1993) is used for convection.

2.2. Urban Canopy Model (UCM)

An Urban Canopy Model (UCM) is coupled with the Noah Land Surface Model (Noah LSM) to run with WRF core (Chen et al., 2006). The purpose of using the UCM is to provide more accurate simulations of the urban regions, and one of the basic functions of the Noah LSM is to provide surface sensible and latent heat fluxes and surface skin temperature as lower boundary conditions for coupled atmospheric models (Chen et al., 2011). The Noah LSM has been enhanced with a simple parameterization for urban land use (Liu et al., 2006). This includes 1) reducing surface albedo from 0.18 to 0.15 to represent the shortwave radiation trapping in the urban canyons, 2) increasing the roughness length from 0.5 to 0.8 m to represent turbulence generated by roughness elements and drag from buildings, 3) a larger volumetric heat capacity of 3.0×10^6 J m^{-3} K^{-1} for the urban surface (walls, roads and roofs), 4) increasing the soil thermal conductivity to 3.24 W m^{-1} K^{-1}, and 5) reducing the green vegetation fraction over the urban areas to decrease evaporation (Lo et al., 2007). While this parameterization represents general characteristics of the urban land use, it does improve the model simulation by capturing some important urban features such as modification of land–sea breeze circulation over the PRD region (Chen et al., 2010 and Lo et al., 2007).

2.3. Land-cover data

Two land-cover situations are simulated in the experiments. The control experiment (CTRL) employs the original U.S. Geological Survey (USGS) 24-category vegetation data, which were derived based on the land cover of 1993 (Fig. 2a), representing no urbanization scenario over the PRD region. Another experiment (named URBAN) is simulated with a modified land use map, representing the urban expansion scenario (Fig. 2b). This modification is based on the data of the Planning Department of the Hong Kong SAR Government in 2003 (HKPD, 2003).

2.4. Weekly mean Optimum Interpolation (OI) sea surface temperature

Weekly mean Optimum Interpolation (OI) version 2 SST data on a $1^\circ \times 1^\circ$ grid obtained from the National Oceanic and Atmospheric Administration are used as boundary conditions for the model simulation.

2.5. Model simulation

To determine the urbanization impacts on the regional climate in different seasons, the experiments are designed to simulate the conditions in both summer (June to August, JJA) and winter (December to February, DJF). To study the possibility of interannual variability, the model is run for 26 years from 1984 to 2009, each with 8 ensemble members initialized with a fixed lag of 6 h from the starting time of the previous member. For each year, the model is initiated from 0000UTC on 1 May and run to 0000UTC on 1 September for the summer run and from 0000UTC on 1 November to 0000UTC on 1 March of the following year for the winter run. Analyses of the results are made for the average for JJA and DJF, with the first month of each run being considered as the spin-up period for the model.

Taking advantage of the fact that the NNR is insensitive to surface observations over land (Kalnay and Cai, 2003), the CTRL run is considered as the control experiment, which represents the

situation that does not have any urbanization over the PRD region. For the URBAN run, the land cover has considerable increase in urban area over the PRD region compared with the USGS land cover data. Therefore, the URBAN run represents the urban expansion scenario. The differences in simulated results between URBAN and CTRL are considered as the impacts on climate due to urbanization.

2.6. The unified monsoon index (UMI)

One important synoptic forcing of the climate in the PRD is the monsoon. To study the relative importance between the monsoon forcing and urbanization effects, the magnitude of the former for a particular year or season is quantified by the unified monsoon index (UMI) defined by Lu and Chan (1999). The UMI for summer and winter are derived from the averaged value of monthly meridional wind (v) fields at 1000 hPa over the South China Sea (7.5° – 20°N, 107.5° – 120°E) from June to August (JJA) and November to February (NDJF) respectively. The advantage of using the UMI is that it is applicable for both summer and winter monsoons in the targeted region. The sign of the UMI indicates the wind direction, negative for northerly and positive for southerly and the magnitude of the UMI indicates the strength of the monsoon.

2.7. ENSO index

Another important synoptic forcing is ENSO. Oceanic Niño Index (ONI) is used as the index of ENSO in the current study. ONI is defined as 3-month running mean of the Extended Reconstructed Sea Surface Temperature (ERSST.v3b) anomaly (SSTA) in the Nino-3.4 region (5°S–5°N, 170°–120°W).

3. Model validation

To examine the performance of the model, the pattern correlation coefficient (r) for the model is computed to quantify the spatial correlation between the model and NNR deviations from the variable mean. Pattern correlation coefficient (centered) for simulated variables is defined as the correlation between the simulation and observed variables (Wilks, 2006)

$$r = \frac{\sum(S-\bar{S})(N-\bar{N})}{\sqrt{\sum(S-\bar{S})^2}\sqrt{\sum(N-\bar{N})^2}}$$

The deviations of the simulated (S) and NNR (N) variables are calculated from the difference in variables of each year and variable mean of simulated ($\bar{S}$) and NNR ($\bar{N}$), respectively. The score ranges from −1 to 1, with 1 being the perfect score. According to Wilks (2006), values of $r = 0.5$ and $r = 0.6$ are generally used as the reference values for evaluation, with $r = 0.6$ representing a reasonable lower limit for delimiting field forecasts that are synoptically useful.

Table 1 shows the climatological mean of monthly r of different surface variables. The model performs well in simulating T2 in both summer and winter compared to NNR. The verification score of T2 in summer and winter are 0.706 (standard deviation, SD, = 0.037) and 0.9806 (SD = 0.0020), respectively. The model also performs quite well in simulating the latent heat flux (LH) in winter ($r = 0.812$ and SD = 0.025). However, r is only 0.54 (SD = 0.10) for the summer which is below 0.6, but it is still greater than 0.5 (>95% confidence). An examination of the model performance in simulating the 10-m winds shows that the model gives less accurate simulations in the summer than in the winter. For the summer, the correlation coefficients of V10 and U10 are just 0.69 (SD = 0.14) and 0.65 (SD = 0.19), respectively. The total precipitation in JJA and DJF over the interested area (21°–24.5°N, 111°–116°E) is also examined. Though the model performance of simulating precipitation varies with years, simulation of winter precipitation ($r = 0.60$, SD = 0.24) is more accurate than that of summer in general, as expected. The model did not perform well in summer, which r is 0.31 (SD = 0.17), especially during most of the El Niño years. A possible reason is a greater rainfall anomaly over the coastal region in El Niño years due to the strengthened atmospheric circulation over the northern part of the South China Sea (Wu et al., 2003).

Table 1
The climatological mean of monthly pattern correlation coefficient and standard deviation (SD) of 2-m temperature (T2), latent heat flux (LH), 10-m meridional wind (V10) and 10-m zonal wind (U10) in summer and winter. Other than LH in summer, the result is significantly greater than the reference level ($r = 0.6$) with 90% confidence.

	JJA		DJF	
	Monthly mean	SD	Monthly mean	SD
T2	0.706	0.037	0.9806	0.0020
LH	0.54	0.10	0.812	0.025
V10	0.69	0.14	0.813	0.044
U10	0.65	0.19	0.833	0.028

Overall, the simulated variables bear a high similarity to the NNR which imply that the model is able to capture most of the surface features in the simulations.

4. Result and discussion

4.1. Effects on thermodynamic parameters

To determine the urbanization effects on the variables, the differences in simulated results between URBAN and CTRL (hereafter, "delta", Δ) are computed.

4.1.1. Urban warming

Urban warming is well documented and one of the indicative phenomena observed in cities. Lam (2006) found at the center of Hong Kong an increase in annual mean temperature with a rate of 0.37 °C per decade during 1989 and 2005, which was largely due to urbanization in Hong Kong. Also, by comparing the daily mean temperature data for weather stations and the NNR between 1980 and 1999, Zhang et al. (2005) obtained an increasing trend of 0.4–0.8 °C (10 year)$^{-1}$ in the entire PRD region due to land use changes.

Urban warming is therefore one of the obvious and expected results obtained in the current study. The climatological mean of ΔT2 in JJA and DJF (Fig. 3) shows that the T2 in URBAN is greater than that in CTRL by 0.8–1.2 °C and 0.1–0.3 °C in the urban area for JJA and DJF, respectively. To compare the changes between summer and winter, the percentage change of T2 (%T2) is calculated as (URBAN − CTRL)/CTRL. The %T2 is 4.25 (SD = 0.33) % and 1.64 (SD = 0.42) % in the urban area for JJA and DJF, respectively. The results show that the urban warming effect is greater in summer than in winter which implies that the UHI effect is stronger in summer over the PRD region.

The result is consistent with previous studies that the temperature increases over the PRD region due to urbanization. Moreover, the magnitude of temperature increase in current study falls within the range of warming trend observed by Zhang et al. (2005).

4.1.2. Surface heat fluxes and 2-m relative humidity

The impacts on the other surface variables due to urbanization are also notable. Table 2 shows the urban-averaged differences

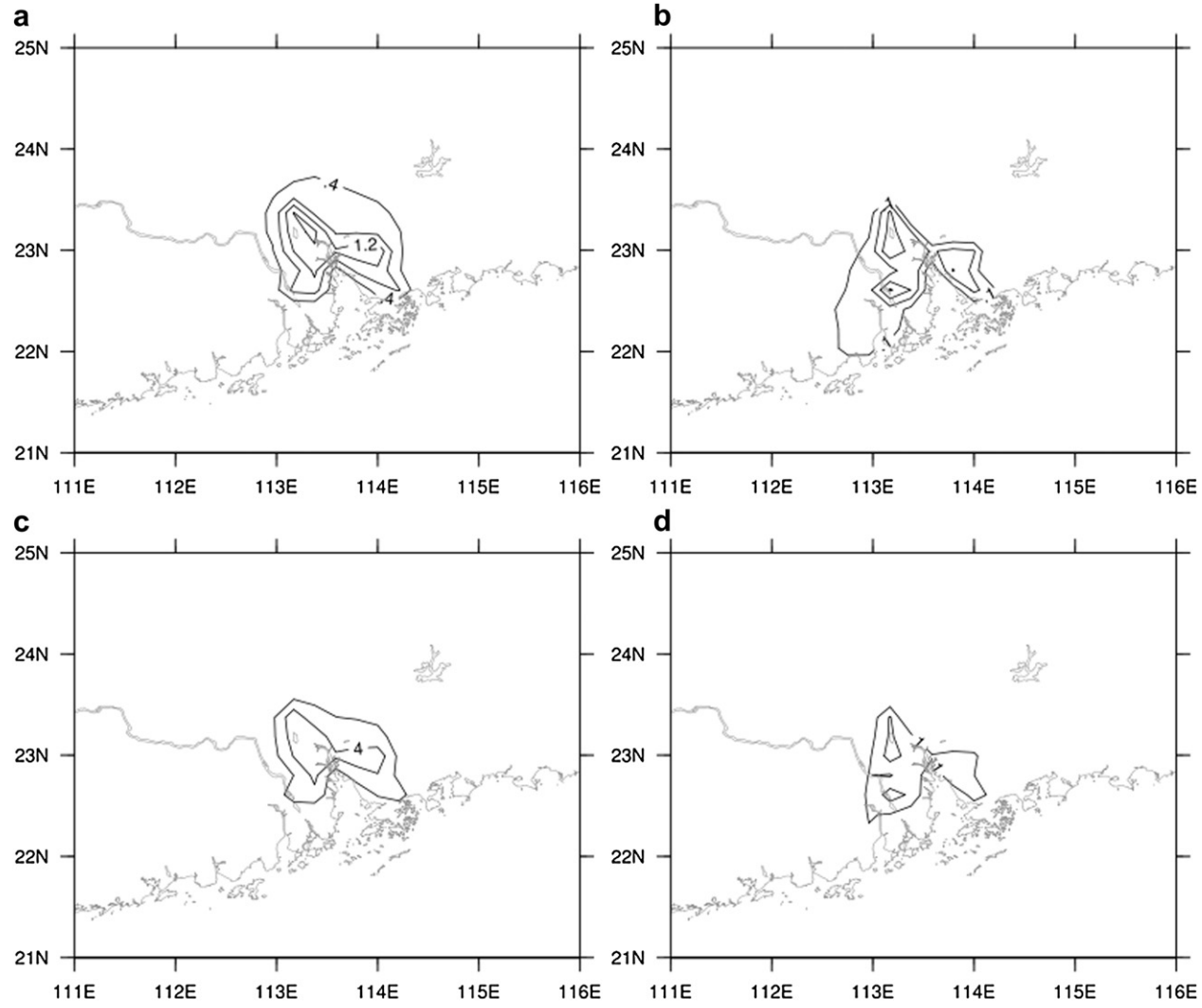

Fig. 3. The climatological mean of 2-m temperature difference between URBAN and CTRL (ΔT2) in a) JJA and b) DJF; and percentage change between URBAN and CTRL in c) JJA and d) DJF. Contour interval: a) 0.4 °C, b) 0.1 °C, c) 2% and d) 1%.

(URBAN − CTRL) in T2, LH, sensible heat flux (SH) and 2-m relative humidity (RH2) in summer and winter. The percentage change of variables is also calculated. The results agree with Lin et al. (2010) who found that urban-averaged latent heat flux and sensible heat flux changed by −68% (ΔLH = −87 W m^{-2}) and +200% (ΔSH = 28.5 W m^{-2}) respectively over the PRD region in October 2004.

Consistent urban effects are found on the surface variables in summer and winter. Increases in T2 and SH while reductions in LH and RH2 are found due to urbanization in both JJA and DJF. As the key principle of determining the dynamics and thermodynamics above the surface, the changes of surface energy balance provide an explicit explanation of urbanization effect by local forcing (Piringer et al., 2002). The ΔSH is 76.1 (SD = 5.2) and 15.6 (SD = 3.1) W m^{-2} in JJA and DJF, respectively. On the other hand, ΔLH is −111.4 (SD = 5.8) and −19.5 (SD = 4.1) W m^{-2} in JJA and DJF, respectively. RH2 is also found to have a negative change of −11.21 (SD = 0.87) % in summer and −3.98 (SD = 0.74) % in winter. The changes in SH

Table 2
The urban-averaged differences (URBAN − CTRL) and standard deviation (SD) in 2-m temperature, surface latent heat flux, sensible heat flux and 2-m relative humidity in JJA and DJF. The percentage change is calculated by (URBAN − CTRL)/CTRL. Urban-averaged value is the average of the area that defined as urban/built-up land over the PRD in the simulation. All result in the table is significant with 95% confidence.

	Urban-averaged difference				Percentage Change (%)			
	JJA		DJF		JJA		DJF	
	Urban-averaged difference	SD	Urban-averaged difference	SD	Urban-averaged difference	SD	Urban-averaged difference	SD
2-m temperature (°C)	1.230	0.089	0.266	0.071	4.25	0.33	1.64	0.42
Surface latent heat flux (Wm^{-2})	−111.4	5.8	−19.5	4.1	−85.6	1.1	−79.83	0.70
Surface sensible heat flux (Wm^{-2})	76.1	5.2	15.6	3.1	168	33	51	17
2-m relative humidity (%)	−11.21	0.87	−3.98	0.74	−14.87	0.85	−5.57	0.81

and LH mainly result from the increased shortwave absorption and reduced longwave emission in cities.

In term of the percentage change, T2 increases in the summer by 4.25 (SD = 0.33) % and 1.64 (SD = 0.42) % in the winter time in URBAN (>95% confidence). Moreover, difference in SH between the URBAN and CTRL is larger in the summer, with an increase of 168 (SD = 33) % but only 51 (SD = 17) % in winter. As for the %LH and %RH2, the changes in the summer are also significantly greater than those in the winter. Therefore, the results further indicate that the urbanization impacts on the climate over the PRD region have its seasonal variations, and that the urbanization effects in the summer time is more pronounced. The result also agrees with a previous study on Yangtze River Delta, which is also a subtropical climate region located in southeast China, that strongest urbanization impacts on climate are found in summer (Zhang et al., 2010). The stronger influences on the thermodynamic field in summer are mainly caused by the greater modification of surface radiation parameters of the urban land use.

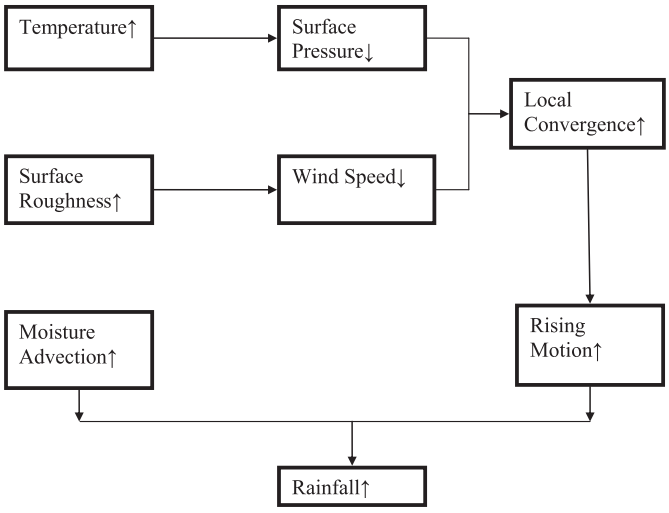

Fig. 5. Schematic diagram of the hypothesized mechanism of urbanization impacts on summer rainfall.

4.2. Effects on precipitation

The complicated effects on rainfall brought by local and synoptic forcing lead to uncertainties of rainfall prediction. In urban areas, less vegetation leads to greater surface sensible heat which enhances convective circulation over the region. However, reduced vegetation also decreases the latent heat flux at the surface, and hence reduces the amount of moisture available for cloud formation.

The urbanization impacts on the precipitation in JJA and DJF appear to be different between summer and winter, with the effect

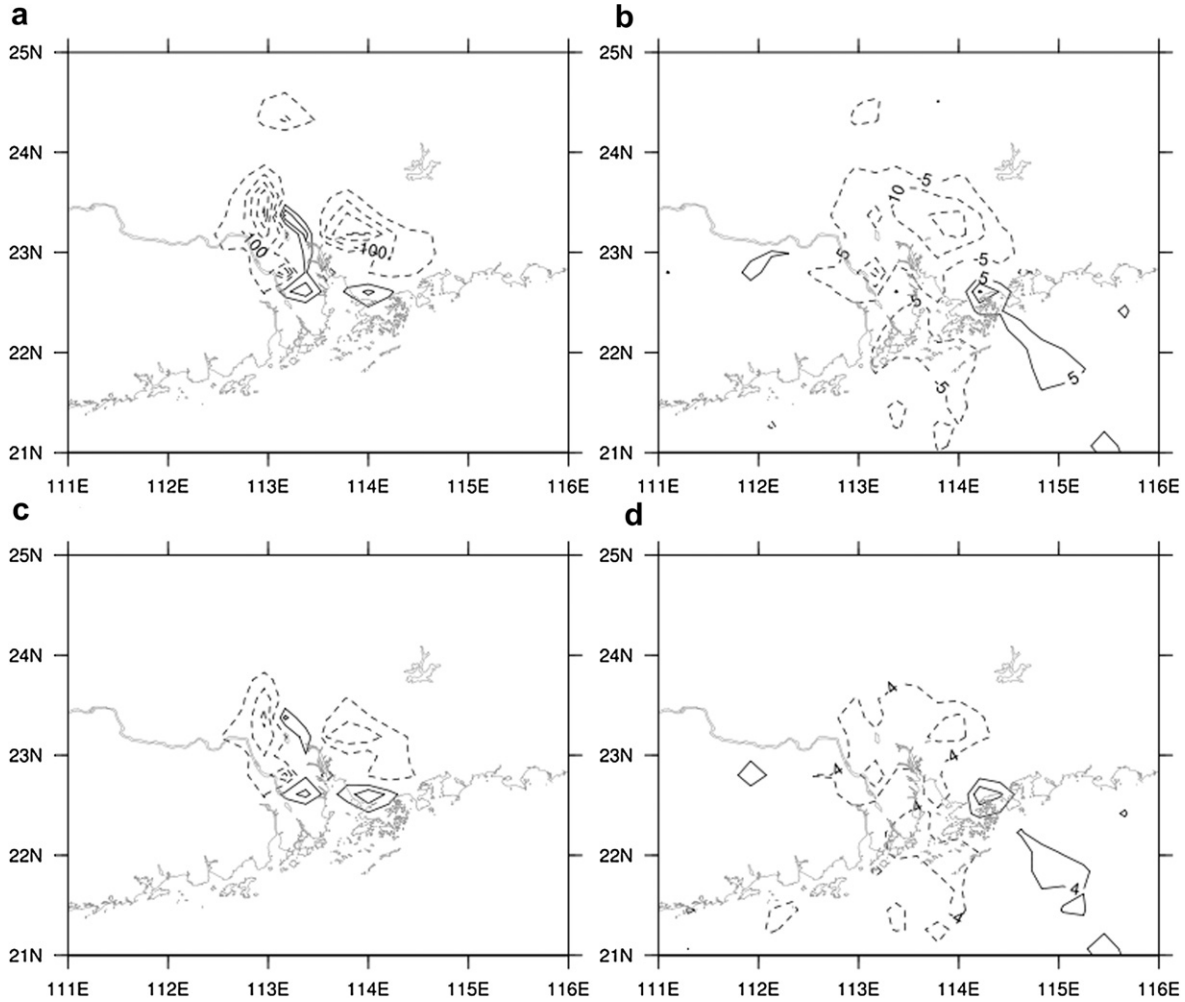

Fig. 4. The climatological mean of precipitation difference between URBAN and CTRL in a) JJA and b) DJF; and percentage change between URBAN and CTRL in c) JJA and d) DJF. Contour interval: a) 50 mm, b) 5 mm, c) 10% and d) 4%. Solid and dashed lines denote positive and negative values respectively.

for summer being significantly greater than that for winter (Fig. 4). In the summer, there is a great reduction in rainfall over the inland urban area, but an increase in rainfall is observed over the coastal region of the urban area. However, in the winter, reduced rainfall is found over the entire urban area. From the seasonal precipitation patterns, it is suggested that different mechanisms likely govern the urbanization impacts on precipitation in the summer and winter. Further analyses are therefore conducted to reveal the underlying processes associated with the urbanization impacts on rainfall in different seasons.

4.2.1. Mechanisms of urbanization impacts on rainfall

The local forcing plays an important role in the precipitation in summer. As mentioned previously, a positive change in T2 is found that in urban area for both summer and winter. And the urbanization impacts on the surface variables are more pronounced in summer. The strength of UHI effect should therefore be stronger in the summer. Fig. 5 shows the schematic diagram of the hypothesized mechanism of urbanization impacts on summer rainfall. It is suggested that the changes of land-cover increases the surface temperature over the urban area so that the urban area becomes

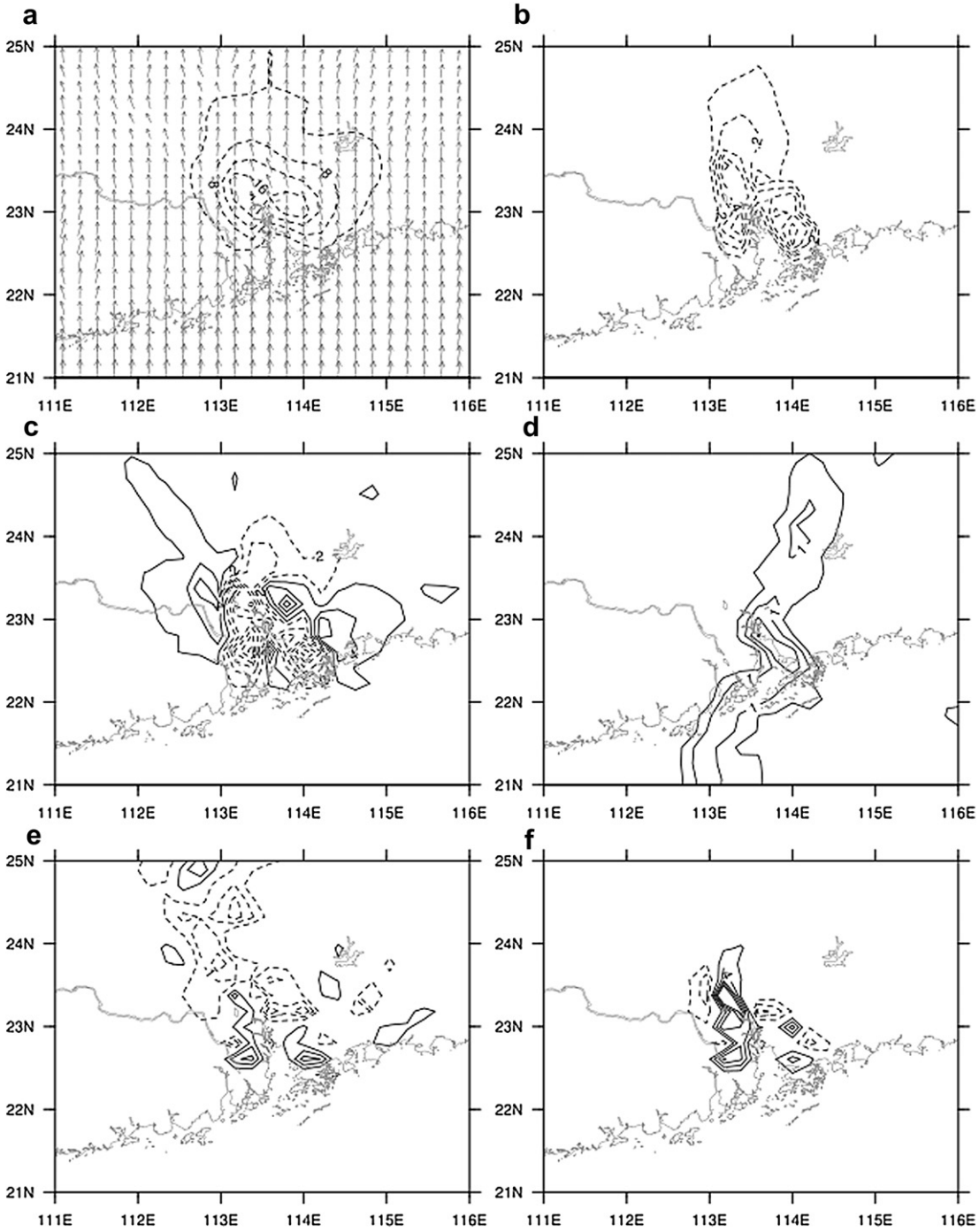

Fig. 6. The climatological mean difference between URBAN and CTRL in JJA of a) surface pressure, b) wind speed at 1000 hPa, c) divergence at 1000 hPa, d) moisture advection at 1000 hPa, e) vertical velocity at 1000 hPa and f) vertical velocity at 850 hPa. In (a), the contour lines show the climatological mean of surface pressure difference between URBAN and CTRL. The vectors show the climatological mean of 10-m wind in URBAN. Contour interval: 4 Pa. Vector reference unit: 3 m s^{-1}. Contour interval for other panels: b) 0.1 $\times$ 10^{-3} m s^{-1}, c) 3 $\times$ 10^{-6} s^{-1}, d) 0.5 $\times$ 10^{-7} kg kg^{-1} s^{-1}, e) 0.5 $\times$ 10^{-3} m s^{-1} and f) 2 $\times$ 10^{-3} m s^{-1}.

a low-pressure area. In addition, increased surface roughness reduces the wind speed over the urban area, hence inducing convergence and rising motion over the urban area. The compensation of moisture brought by the prevailing wind (southerly in summer) contributes to rainfall enhancement over the urban area.

This hypothesis is demonstrated by the numerical model results. The surface pressure over the urban area decreases due to the UHI effect (Fig. 6a). At the same time, the increased surface roughness reduces the wind speed over the urban area (Fig. 6b). Surface convergence over the urban area therefore increases over the urban area (Fig. 6c). Southerly wind brings moisture to the urban area from the sea. The increase in rainfall over the coastal area can be explained by the strong positive moisture advection over that region. The compensation of moisture from the sea contributes to the major rainfall enhancement over the urban area in summer. The increased low-level vertical velocity over the urban area shows an enhancement in convection (Fig. 6d and e). As a result, urban rainfall enhancement is observed. The non-uniform precipitation change pattern may also explain why some previous statistical studies claim a negative impact on precipitation by urbanization. It is because rainfall enhancement can only found over the coastal region and the center of the PRD region.

Reduced precipitation is, however, observed over the urban area in winter. The dry prevailing wind (northeasterly in winter) and the convective stability contribute to the urban rainfall reduction. Wind converges to the windward side and diverges at the leeward side of the urban area (Fig. 7a). However, weaker moisture advection pattern is found in the winter indicating the dry northeasterly wind brings little moisture to the urban area (Fig. 7b). A weakening vertical velocity at 850 hPa over the urban area indicates unfavorable conditions for rainfall (Fig. 7c). As a consequence, negative impact on winter precipitation is found in most of the urban areas.

4.2.2. Local vs. synoptic forcing

Because the synoptic forcing could likely modify the urbanization impacts on the precipitation, the spatial patterns of the precipitation changes are studied in relation to various synoptic forcings, which include ENSO and the monsoons.

It is found that the summer precipitation changes patterns are similar under different synoptic conditions (not shown). From the spatial patterns of the correlation coefficient, no significant relationship can be found between the urbanization impact on summer precipitation and synoptic forcing (not shown). In other words, the strong local forcing possibly dominates over the synoptic forcing in

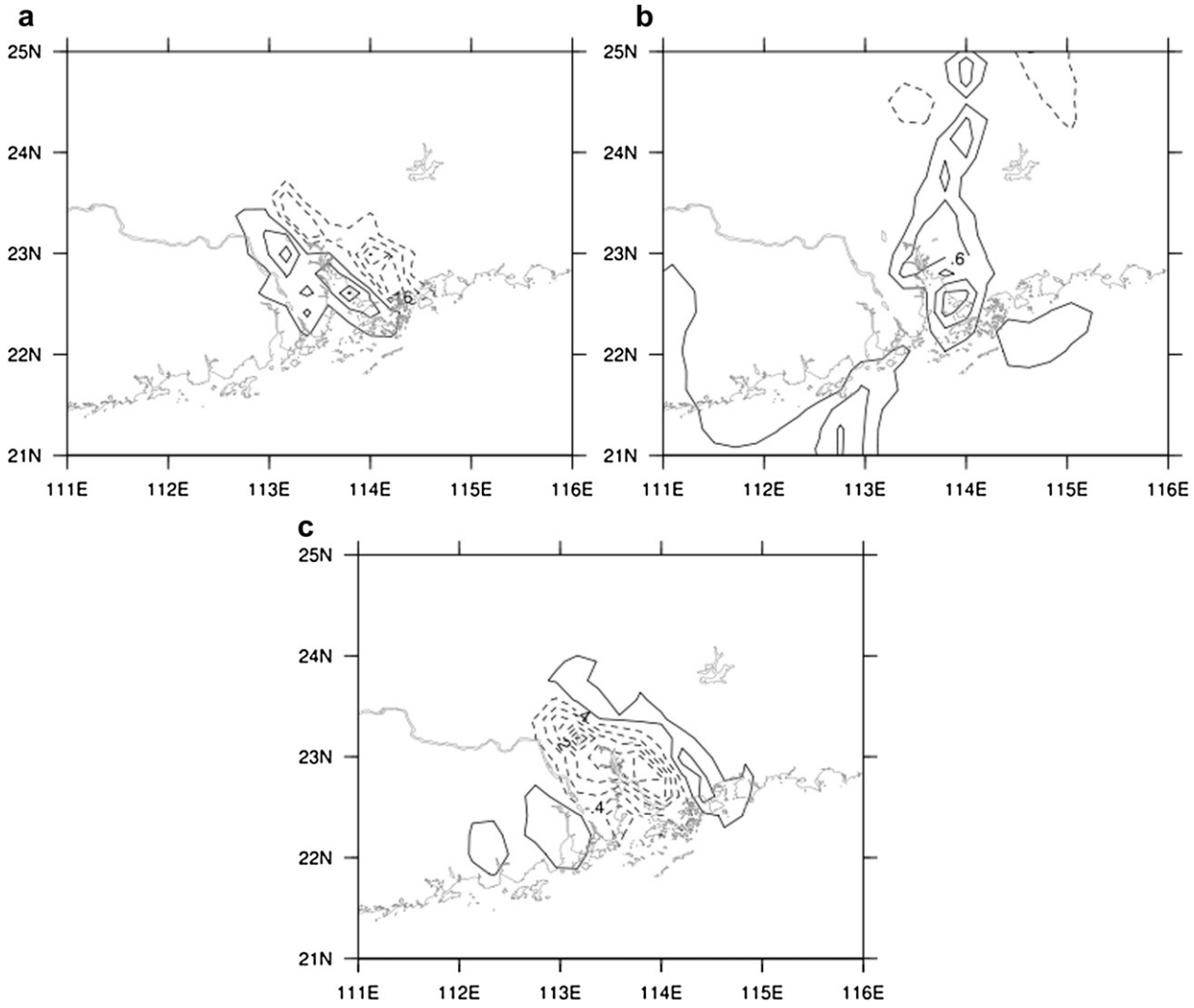

Fig. 7. The climatological mean difference between URBAN and CTRL in DJF of a) divergence at 1000 hPa, b) moisture advection at 1000 hPa, c) vertical velocity at 850 hPa. Contour interval: a) 4×10^{-6} s^{-1}, b) 0.3×10^{-7} kg kg^{-1} s^{-1}, c) 0.5×10^{-3} m s^{-1}.

summer. However, interaction between winter precipitation and synoptic forcing is observed, as the UHI effect in winter is weaker than that in summer.

4.2.3. Relationship between ENSO and urban rainfall

Influence of ENSO on winter rainfall over the PRD region has been found to be significant. For example, due to a significant moisture convergence and ascent motion, winter rainfall over PRD increases during El Niño years (Zhou et al., 2010; Wu et al., 2003). In the current study, the precipitation changes are classified into various ENSO conditions (warm, moderate and cold years). The strength of ENSO is determined by the ONI for JJA and DJF. Based on the operational definition from National Oceanic and Atmospheric Administration (NOAA), a warm (cold) episode is one when the ONI is $>0.5\ ^{\circ}C$ ($<0.5\ ^{\circ}C$) for a minimum of five consecutive overlapping seasons. Therefore, a warm (cold) summer or winter year is defined as the year when a warm (cold) episode occurred in JJA or DJF. Moreover, a moderate year is defined as the year is neither warm nor cold year. The change in precipitation is negatively correlated with the ENSO index over the windward (northeastern) side of the urban area, but positively correlated over the coastal area (Fig. 8a). In other words, greater urban rainfall enhancement may be observed in the warmer years over the coastal region. To determine changes in precipitation under various ENSO conditions, the three ENSO conditions are further grouped into warm–moderate (includes warm and moderate years) and cold–moderate (includes cold and moderate years) ENSO conditions. A close relationship is found between ENSO and urban rainfall in winter under warm–moderate ENSO condition (Fig. 9). However, the change in urban rainfall has no significant correlation with the strength of ENSO under cold–moderate ENSO condition (not shown).

According to the Hong Kong Observatory, impacts of El Niño and La Niña on the climate of Hong Kong are observed. In winter, El Niño brings more rainfall to the coastal region and La Niña strengthens the northeast monsoon bringing a lower temperature

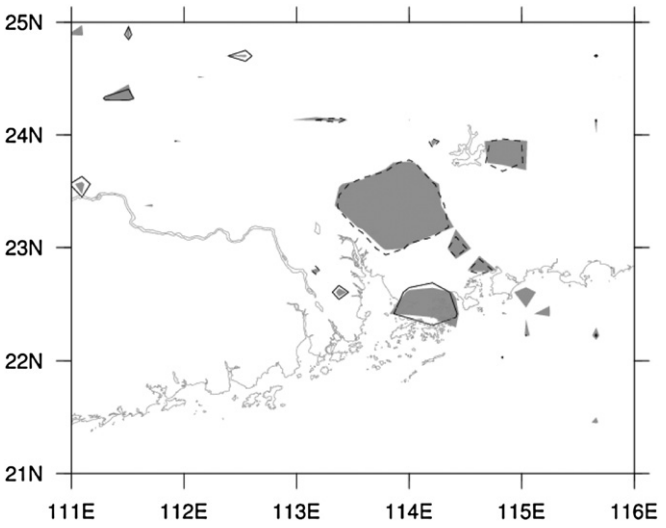

Fig. 9. Correlation of precipitation difference with warm–moderate ENSO condition in DJF. Contour interval: 0.2. The shading denotes regions with correlation at 95% confidence.

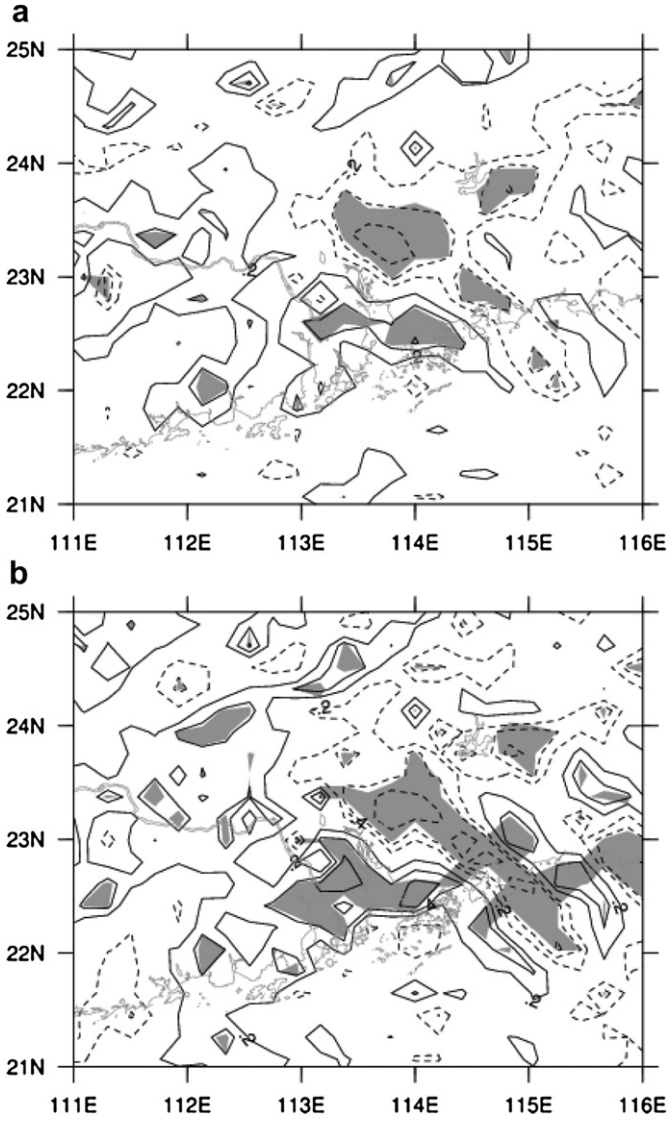

Fig. 8. Correlation of precipitation difference between URBAN and CTRL with a) ENSO index and b) UMI in DJF. Contour interval: 0.2. The shading denotes regions with correlation at 95% confidence.

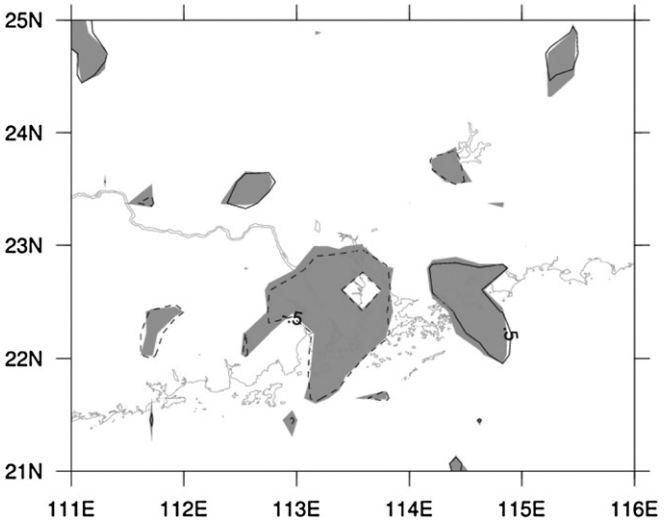

Fig. 10. Correlation of moisture advection difference at 850 hPa with warm–moderate ENSO condition in DJF. Contour interval: 0.2. The shading denotes regions with correlation at 95% confidence.

to Hong Kong than in the moderate year (Wu and Leung, 2008). Therefore, the Δmoisture advection is probably also affected by ENSO. Fig. 10 shows that Δmoisture advection correlated with the ENSO index under warm–moderate ENSO condition. A positive correlation is observed over the windward (eastern and northern) region of the urban area. The result suggests that a strengthening moisture advection at 850 hPa brings more moisture to the urban area in El Niño. However, the relationship between Δmoisture advection and La Niña is unnoticeable. A weak pattern of increased convergence over the urban area is also found under warm–moderate ENSO condition (not shown), but not under cold–moderate ENSO condition. Moreover, the ΔT2 is also independent of the ENSO conditions, neither in the warm–moderate nor cold–moderate years (not shown). Therefore, it is suggested that the urban effects on thermodynamic parameters are independent of the synoptic forcing, but determined by the local forcing even in the winter. That implies that the association of changes in urban rainfall and ENSO effects could mainly due to the changes in moisture advection and modification of the atmospheric circulation.

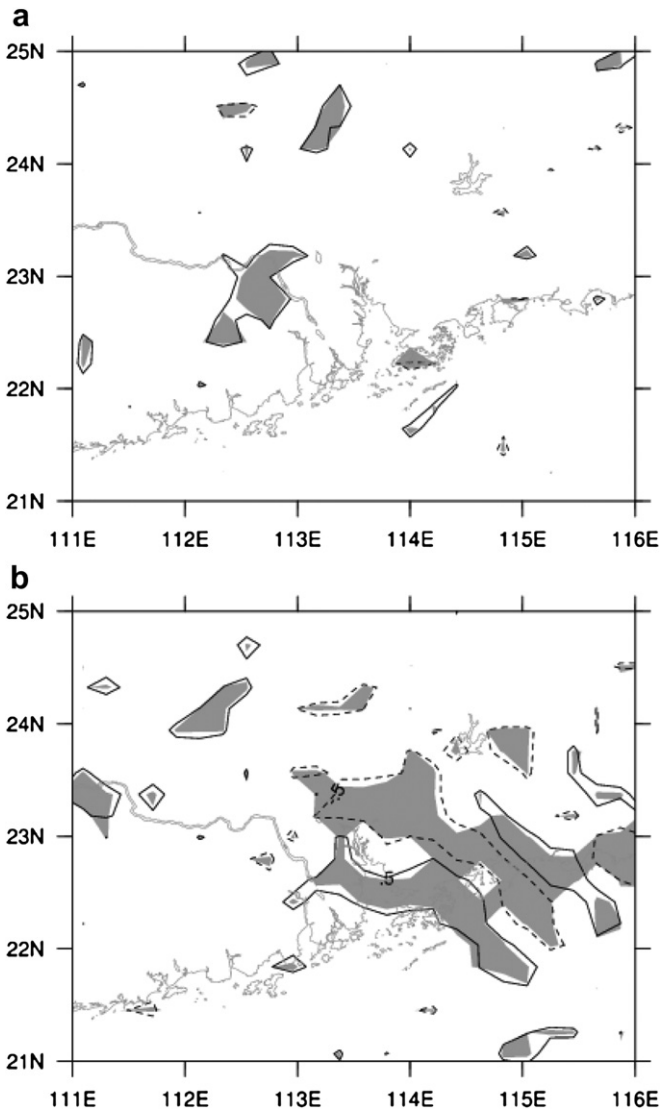

Fig. 11. Correlation of precipitation difference with a) strong–normal and b) weak–normal monsoon condition in DJF. Contour interval: 0.2. The shading denotes regions with correlation at 95% confidence.

4.2.4. Relationship between monsoon and urban rainfall

The urban rainfall and the winter monsoon are significantly correlated (correlation coefficient > 0.6 with 95% confidence). In the current study, the 26 years are also classified into three categories (strong, normal and weak monsoon years) according to the strength of monsoon in that year. A strong and weak monsoon year are defined by year with UMI greater than −4.89 (66.6th percentile) and lower than −4.53 (33.3rd percentile) in magnitude respectively. Years with UMI between −4.89 and −4.53 are classified as normal monsoon years. To investigate the influence of Δprecipitation under various monsoon conditions, the three monsoon conditions are further grouped into strong–normal (includes strong and normal monsoon years) and weak–normal (includes weak and normal monsoon years) monsoon conditions for investigating the extreme conditions.

The urban rainfall is also conditional on the strength of the winter monsoon (Fig. 11). The monsoon effect further explains how the synoptic forcing alters the dynamics of regional climate, resulting in changes in urban rainfall. Similar to the ENSO effects, there is no significant relationship observed between strong monsoon condition and urban rainfall. However, a notable correlation is observed under weak and normal monsoon condition. This implies that the effect of winter monsoon is maximized when the winter monsoon is strong. The urban rainfall is then affected by other forcings. When the winter monsoon is weak, the Δprecipitation pattern is then the net effects of other forcing, including local forcing and synoptic forcing such as ENSO. No significant correlation between monsoon strength and the Δmoisture advection and Δdivergence can be observed under strong monsoon conditions (not shown). On the other hand, under weak–normal condition, convergence increases with monsoon strength (Fig. 12). However the stronger dry northeasterly wind decreases the moisture over the windward region (Fig. 13) and hence leads to more urban rainfall reduction.

Because the UHI effect in winter is not as strong as that in summer, it is likely that the interaction between synoptic forcing and urbanization effect on the winter precipitation would be more noticeable. From Fig. 8, the changes of winter precipitation are significantly associated with the synoptic forcings. The result suggests that a strong synoptic flow reduces the urbanization effects over the urban area. It is emphasized that the changes in thermodynamic parameters such as T2 are independent of the

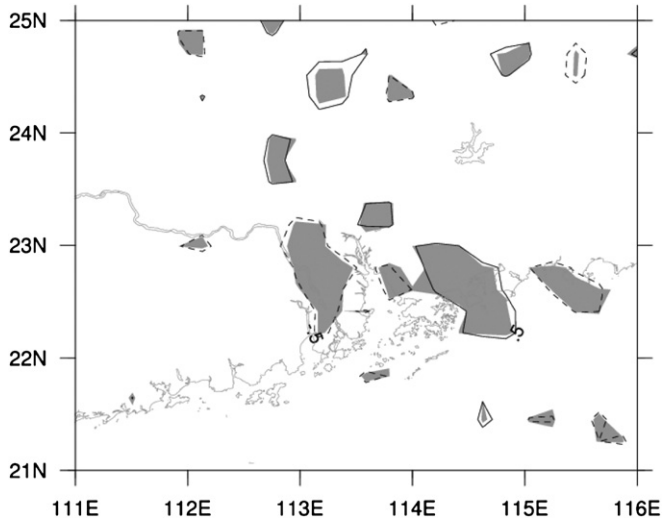

Fig. 12. Correlation of divergence difference at 1000 hPa with weak–normal monsoon condition in DJF. Contour interval: 0.2. The shading denotes regions with correlation at 95% confidence.

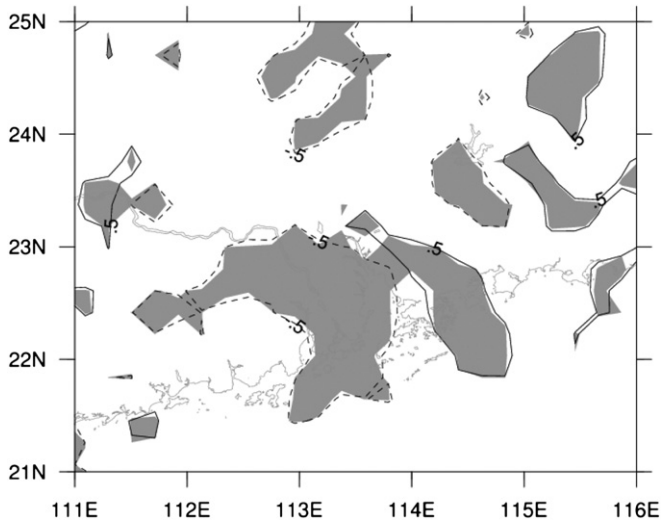

Fig. 13. Correlation of moisture advection difference at 850 hPa with weak–normal monsoon condition in DJF. Contour interval: 0.2. The shading denotes regions with correlation at 95% confidence.

synoptic forcing. And the major linkage between the changes in urban rainfall and synoptic forcing would be the modification of the dynamic features.

The non-uniform precipitation change pattern still can be observed, from the spatial patterns of the correlation coefficient. Different urban regions are sensitive to various synoptic forcing. The coastal area is always found to be sensitive to the synoptic forcing. In the weak monsoon and warm ENSO years, positive moisture advection is observed over the coastal area. It is probably because of the weakening of the dry northerly wind, which encourages moist sea air flowing towards the coastal area.

5. Summary and conclusion

In the current study, the seasonal variations of urbanization impacts on climate over the PRD are investigated. Urban warming and modifications of surface variables (T2, SH, LH and RH2) are observed in both summer and winter. The urbanization effects are greater in summer than these in winter. The pattern of precipitation changes is also studied and the detailed mechanism of urbanization impact on rainfall is also hypothesized. Increased summer rainfall, however, reduced winter precipitation is found in the study. All changes are induced by urbanization, but processes that cause the changes vary depending upon large-scale conditions. Therefore, under weak synoptic flow conditions, local thermodynamic effects of urbanization dominate, setting up convergence zone over the urban area and leading to increased precipitation. However, during winter time, under the influence of strong northeasterly synoptic flow, dynamic effects of increased surface roughness over the urban areas dominate and lead to convergence upwind of the urban region. In other words, the increased summer rainfall is mainly because of the strong local forcings that impacts on the thermodynamic parameters, while the reduced winter precipitation is due to the dominating synoptic flow which changes the dynamic processes of the urbanization effects.

6. Future work

The impacts of land-cover changes such as increase in roughness length, reduction in albedo and vegetation fraction, on the regional climate over the PRD have been studied. However, other important urbanization characteristics such as increase in anthropogenic heat (AH) and air pollution are not considered in the current study. The seasonal variation of AH and air pollution problems have been suggested to have a close relationship with urban rainfall (Wang et al., 2011; Oke et al., 1991). Therefore, future research will include a determination of how these factors may impact on the regional climate over the PRD.

Acknowledgments

This is from part of the first author's PhD work, which is supported by the Research Studentship of City University of Hong Kong. The authors wish to thank the valuable comments from the two reviewers.

References

Castro, C.L., Pielke Sr., R.A., Leoncini, G., 2005. Dynamical downscaling: assessment of value retained and added using the Regional Atmospheric Modeling System (RAMS). J. Geophys. Res. 110 (D5), D05108. http://dx.doi.org/10.1029/2004JD004721.

Chen, F., Manning, K.W., LeMone, M.A., Trier, S.B., Alfieri, J.G., Roberts, R., Wilson, J., Tewari, M., Niyogi, D., Horst, T.W., Oncley, S.P., Basara, J., Blanken, P., 2006. Description and Evaluation of the characteristics of the NCAR high-resolution land data assimilation system. J. Appl. Meteor. Climatol. 46, 694–713.

Chen, J., Li, Q.L., Niu, J., Sun, L.Q., 2010. Regional climate change and local urbanization effects on weather variables in Southeast China. Stochastic Environmental Research & Risk Assessment. http://dx.doi.org/10.1007/s00477-010-0421-0.

Chen, F., Kusaka, H., Bornstein, R., Ching, J., Grimmond, C.S.B., Grossman-Clarke, S., Loridan, T., Manning, K.W., Martilli, A., Miao, S., Sailor, D., Salamanca, F.P., Taha, H., Tewari, M., Wang, X., Wyszogrodzki, A.A., Zhang, C., 2011. The integrated WRF/urban modelling system: development, evaluation, and applications to urban environmental problems. Int. J. Climatol.. http://dx.doi.org/10.1002/joc.2158

HKPD, 2003. Hong Kong 2030: Planning Vision and Strategy Consultancy Study to Analyse Broad Land Use Pattern of the Pearl River Delta Region, Hong Kong 2030 Forum Final Executive Summary, Technical Paper No. 5, 19 pp.

Huff, F.A., Changnon, S.A., 1972. Climatological assessment of urban effects on precipitation at St. Louis. J. Appl. Meteor. 11, 823–842.

Inoue, T., Kimura, F., 2004. Urban effects on low level clouds around the Tokyo metropolitan area on clear summer days. Geophy. Res. Lett. 31, L05103.

Kain, J.S., Fritsch, J.M., 1993. Convective parameterization for mesoscale models: the Kain–Fritsch scheme. The representation of cumulus convection in numerical models. Meteor. Monogr. 24, 165–170.

Kalnay, E., Cai, M., 2003. Impact of urbanization and land use on climate change. Nature 423, 528–531.

Kaufmann, R.K., Seto, K.C., Schneider, A., Liu, Z., Zhou, L., Wang, W., 2007. Climate response to rapid urban growth: evidence of a human-induced precipitation deficit. J. Clim. 20, 2299–2306.

Kishtawal, C.M., Niyogi, D., Tewari, M., Pielke Sr., R.A., Shepherd, M., 2009. Urbanization signature in the observed heavy rainfall climatology over India. Int. J. Climatol. 30, 1908–1916.

Lam, C.Y., 2006. On Climate Changes Brought About by Urban Living. HKO Reprint No. 700. Hong Kong Observatory, 9 pp.

Lin, W., Wang, B., Li, J., Wang, X., Zeng, L., Yang, L., Lin, H., 2010. The impact of urbanization on the monthly averaged diurnal cycle in October 2004 in the Pearl River Delta region. Atmosfera 23 (1), 37–51.

Liu, Y., Chen, F., Warner, T., Basara, J., 2006. Verification of a mesoscale data-assimilation and forecasting system for the Oklahoma City area during the Joint Urban 2003 Field Project. J. Appl. Meteorol. 45, 912–929.

Lo, J.C.F., Lau, A.K.H., Chen, F., Fung, J.C.H., Leung, K.K.M., 2007. Urban modification in a mesoscale model and the effects on the local circulation in the Pearl River Delta region. J. Appl. Meteor. Climatol. 46, 457–476.

Lu, E., Chan, J.C.L., 1999. A unified monsoon index for South China. J. Clim. 12, 2375–2385.

NASA Landsat Program, 19/10/1979. Landsat MSS Scene p131r44_3m19791019, Orthorectified. USGS, Sioux Falls.

NASA Landsat Program, 14/09/2000. Landsat ETM+ Scene p122r044_7t20000914, Orthorectified. USGS, Sioux Falls.

Niyogi, D., Pyle, P.C., Lei, M., Arya, S.P., Kishtawal, C.M., Shepherd, J.M., Chen, F., Wolfe, B., 2011. Do urban areas modify thunderstorms? – an observational storm climatology and model case study for the Indianapolis urban region. J. Appl. Meteor.Climatol. 150, 1129–1144.

Oke, T.R., Johnson, G.T., Steyn, D.G., Watson, I.D., 1991. Simulation of surface urban heat islands under "ideal" conditions at night part 2: diagnosis of causation. Boundary-Layer Meteorol. 56, 339–358.

Piringer, M., et al., 2002. Investigating the surface energy balance in urban area – recent advances and future needs. Water Air Soil Pollut. Focus 2, 1–16.

Seto, K.C., Kaufmann, R.K., 2009. Impacts of Urban Expansion on Local Precipitation in South China. http://siteresources.worldbank.org/INTURBANDEVELOPMENT/Resources/336387-1256566800920/seto.pdf. 07/01/10.

Shem, W., Shepherd, J.M., 2008. On the impact of urbanization on summertime thunderstorms in Atlanta: two numerical model case studies. Atmos. Res. 92, 172–189.
Skamarock, W.C., Klemp, J.B., Dudhia, J., Gill, D.O., Barker, D.M., Wang, W., Powers, J.G., 2005. A Description of the Advanced Research WRF Version 2. NCAR, Technical Note 468, 88 pp.
Tayanç, M., Toros, H., 1997. Urbanization effects on regional climate change in the case of four large cities of Turkey. Climatic Change 35, 501–524.
UNFPA, 2007. State of the World Population 2007 – Unleashing the Potential of Urban Growth.
Wang, Y., Wan, Q., Meng, W., Liao, F., Tan, H., Zhang, R., 2011. Impacts of aerosols on weather and regional climate over the Pearl River Delta megacity area in China. Atmos. Chem. Phys. Discuss. 11, 23275–23316.
Wilks, D.S., 2006. Statistical Methods in the Atmospheric Sciences, second ed. Academic Press, 627 pp.
Wu, M.C., Leung, W.H., 2008. Effect of ENSO on Winter Monsoon Affecting Hong Kong. HKO Reprint No. 789. Hong Kong Observatory, 15 pp.
Wu, R., Hu, Z.Z., Kirtman, B.P., 2003. Evolution of ENSO-related rainfall anomalies in East Asia and the processes. J. Clim. 16, 3741–3757.
Zhang, J., Dong, W., Wu, L., 2005. Impact of land use changes on surface warming in China. Adv. Atmos. Sci. 22, 343–348.
Zhang, N., Gao, Z., Wang, X., Chen, Y., 2010. Modeling the impact of urbanization on the local and regional climate in Yangtze River Delta, China. Theor. Appl. Climatol. 102, 331–342.
Zhou, L.T., Tam, C.Y., Zhou, W., Chan, J.C.L., 2010. Influence of South China Sea SST and the ENSO on winter rainfall over South China. Adv. Atmos. Sci. 27, 832–844.